Title

A systematic topographical relationship between mouse lateral posterior thalamic neurons and their visual cortical projection targets.

Journal

The Journal of comparative neurology, 528(1)

ISSN

0021-9967

Authors

Juavinett, Ashley L
Kim, Euiseok J
Collins, Hannah C
et al.

Publication Date

2020

DOI

10.1002/cne.24737

Peer reviewed

Received: 12 December 2018 | Revised: 24 June 2019 | Accepted: 25 June 2019

DOI: 10.1002/cne.24737

RESEARCH ARTICLE

JCN RESEARCH IN SYSTEMS NEUROSCIENCE THE JOURNAL OF COMPARATIVE NEUROLOGY WILEY

A systematic topographical relationship between mouse lateral posterior thalamic neurons and their visual cortical projection targets

Ashley L. Juavinett[1,2] | Euiseok J. Kim[1] | Hannah C. Collins[1] | Edward M. Callaway[1]

[1]The Salk Institute for Biological Studies, La Jolla, California

[2]Neurosciences Program UC San Diego, La Jolla, California

Correspondence
Edward M. Callaway, The Salk Institute for Biological Studies, 10010 Torrey Pines Road, La Jolla, CA 93037.
Email: callaway@salk.edu

Present address:
Ashley L. Juavinett, Section of Neurobiology, Division of Biological Sciences, UC San Diego, La Jolla, CA.
Euiseok J. Kim, Department of Molecular, Cell and Developmental Biology, University of California, Santa Cruz, California 95064, USA.

Funding information
National Science Foundation; NIH/NEI, Grant/Award Numbers: EY019005, EY022577; NIH/NIMH, Grant/Award Number: MH063912; The Gatsby Charitable Foundation; The Martinet Foundation

Abstract

Higher-order visual thalamus communicates broadly and bi-directionally with primary and extrastriate cortical areas in various mammals. In primates, the pulvinar is a topographically and functionally organized thalamic nucleus that is largely dedicated to visual processing. Still, a more granular connectivity map is needed to understand the role of thalamocortical loops in visually guided behavior. Similarly, the secondary visual thalamic nucleus in mice (the lateral posterior nucleus, LP) has extensive connections with cortex. To resolve the precise connectivity of these circuits, we first mapped mouse visual cortical areas using intrinsic signal optical imaging and then injected fluorescently tagged retrograde tracers (cholera toxin subunit B) into retinotopically-matched locations in various combinations of seven different visual areas. We find that LP neurons representing matched regions in visual space but projecting to different extrastriate areas are found in different topographically organized zones, with few double-labeled cells (~4–6%). In addition, V1 and extrastriate visual areas received input from the ventrolateral part of the laterodorsal nucleus of the thalamus (LDVL). These observations indicate that the thalamus provides topographically organized circuits to each mouse visual area and raise new questions about the contributions from LP and LDVL to cortical activity.

KEYWORDS
anatomy, lateral posterior nucleus, mouse visual cortex, pulvinar, RRID:MGI:5656552, visual thalamus

1 | INTRODUCTION

While the classic description of the visual system depicts information in parallel streams traveling up a hierarchy of cortical areas, this illustration is complicated by the fact that there is a tremendous amount of feedback to the lateral geniculate nucleus (LGN), as well as to a higher order thalamic nucleus, the pulvinar (Felleman & Van Essen, 1991). While the LGN mainly projects to just the primary visual cortex (V1), primate pulvinar is a relatively large structure that is extensively connected with various areas of visual cortex and is thought to be involved in a variety of behaviors, such as visual attention (specifically, ignoring distractors) as well as visuomotor transduction (Baldwin, Balaram, & Kaas, 2017; Grieve, Acuña, & Cudeiro, 2000; Jones, 1985; Robinson & Petersen, 1992; Saalmann & Kastner, 2011). Studies of the locations of primate pulvinar neurons projecting to different visual cortical areas demonstrate systematic topography that is orthogonal to retinoptopic maps (Shipp, 2001, 2003). Furthermore, the pulvinar also receives visual information from the superior colliculus (Nassi & Callaway, 2009; Stepniewska et al., 2000). Still, our understanding of the contributions of each of these pathways to responses in subcortical and cortical areas and to perception is limited. Investigating pulvinar function would be greatly aided by a more precise map of its

connections in the mouse, where the use of genetic and viral targeting strategies and manipulations are more readily applied.

In cats and rodents, the lateral posterior nucleus of the thalamus (LP) is considered the homolog of primate pulvinar based on its reciprocal connectivity with visual, parietal, and frontal cortex and abundant input from the superior colliculus (Baldwin, Wong, Reed, & Kaas, 2011; Lent, 1982; Nakamura, Hioki, Furuta, & Kaneko, 2015; Raczkowski & Rosenquist, 1983). In rats, hamsters, and squirrels, LP can be divided into several subdivisions (LPLR, LPLC, LPCM, LPMR), based on its cytoarchitecture and connectivity to cortical and subcortical areas (Abramson & Chalupa, 1988; Baldwin et al., 2011; Conte, Kamishina, Corwin, & Reep, 2008; Kamishina et al., 2009; Kamishina, Yurcisin, Corwin, & Reep, 2008; Nakamura et al., 2015; Reep & Corwin, 2009; Sukekawa, 1988; Takahashi, 1985).

Furthermore, LP/pulvinar in rodents, cats, and primates is retinotopically organized, with different subdivisions projecting to retinotopically matched regions of cortex (Bennett et al., 2019; Le Gros Clark, 1932; Mason, 1978; Shipp, 2003; Tohmi, Meguro, Tsukano, Hishida, & Shibuki, 2014). Available evidence indicates that in the mouse, horizontal retinotopy (azimuth) is represented along the medio-lateral axis of mouse LP (Allen, Procyk, Howarth, Walmsley, & Brown, 2016; Roth et al., 2015), while elevation is mapped along the anterior–posterior axis and may consist of two separate mirror-image maps with biases in the inputs to and outputs from the anterior and posterior maps (Bennett et al., 2019). Nevertheless, the central region of LP represents retinotopic locations that overlap between the two maps (Bennett et al., 2019; Tohmi et al., 2014) and may contain neurons projecting to V1 and/or any of the extrastriate cortical areas. The few published accounts of single cell reconstructions suggest that LP neurons often project to more than one cortical region but are likely to be limited in the numbers of visual areas to which they project (Nakamura et al., 2015).

The observation that mouse visual areas have biases in the retinotopic locations they represent (Garrett, Nauhaus, Marshel, & Callaway, 2014; Zhuang et al., 2017) raises new questions about the relationships between retinotopy and projections from LP to each region. In particular, despite known biases in the visual field representations of different extrastriate areas, all areas include a representation with overlap (Garrett et al., 2014). We sought to determine whether there is topographic separation of neurons that project to different extrastriate areas from zones that have retinotopic overlap, as has been previously described for primates (Shipp, 2001). Furthermore, do neurons within the region of mouse LP that represents common visual field locations project indiscriminately to all areas, or might they have more organized projections?

To address these and other questions, we used retinotopic mapping with intrinsic signal imaging to target cortical injections of retrograde tracers to retinotopically matched locations within multiple extrastriate cortical areas of single animals; matching of retinotopic injections was further verified based on overlapping retrograde label in V1, which contains a nearly complete retinotopic map (Garrett et al., 2014; Zhuang et al., 2017). We find that projections to extrastriate areas reveal a third dorso-ventral topographic axis within LP, roughly orthogonal to the A-P and M-L axis representations of visual space. LP neurons located more dorsally project to more posterior visual cortical areas, while more ventral neurons project to more anterior areas; these topographic relationships are gradual and systematic such that intermediate visual cortical areas receive input from intermediate LP locations. Furthermore, even within regions of overlap, very few LP neurons are double-labeled, suggesting that they make relatively dedicated cortical projections. These data shed light on whether LP serves to pass information up the cortical hierarchy, or rather acts as a loop within various visual areas and contribute to growing evidence providing a framework against which various theories of thalamocortical circuit function can be evaluated (Crick & Koch, 1998; Grieve et al., 2000; Olshausen, Anderson, & Van Essen, 1993; Sherman & Guillery, 1998).

In addition to LP, the lateral dorsal nucleus of the thalamus (LD) is yet another "higher order" thalamic nucleus that has connections to various pathways including visual, limbic, and somatosensory (Bezdudnaya & Keller, 2008; Jones, 1985; Robertson & Kaitz, 1981; Takahashi, 1985). In the rat, the ventral lateral part of this nucleus (LDVL) receives input from both primary and secondary visual cortex, while the medial portion does not (Takahashi, 1985). Beyond this tracing study, there is remarkably little research on involvement of this relatively large nucleus in visual circuits. We find that like LP, LD also projects to all visual cortical areas in the mouse.

2 | MATERIALS AND METHODS

2.1 | Headframe implantation and intrinsic signal optical imaging

All experimental procedures using live animals followed procedures approved by the Salk Institute Animal Care and Use Committee. C57BL/6 mice (RRID:MGI:5656552) (5–14 weeks old, 2 mice less than 6 weeks old) were prepared for imaging by implanting a custom metal headframe as previously described (Figure 1; Marshel, Garrett, Nauhaus, & Callaway, 2011; Garrett et al., 2014; Juavinett, Nauhaus, Garrett, & Callaway, 2017). These headframes remained on the mouse for the remainder of the experiment. Before injection, a map of visual cortex was obtained for each mouse using intrinsic signal optical imaging as previously described (Garrett et al., 2014; Juavinett et al., 2017; Sereno, Mcdonald, & Allman, 1994). Using this mapping protocol, we were able to reliably target seven different visual areas (V1, LM, RL, AL, AM, PM, and P/POR). Although visual area A receives inputs from V1, it is not retinotopically mapped and was therefore not targeted in our study (Garrett et al., 2014; Wang & Burkhalter, 2007).

2.2 | Cholera toxin subunit B injection

To trace inputs to visual cortical areas from the thalamus, we used 0.5% in filtered PB of Cholera Toxin Subunit B (CTB) conjugated to Alexa-Fluor (AF) 488, 555, or 647 (Life Technologies; AF-CTB). We found that the different AF-CTB performed comparably. The choice

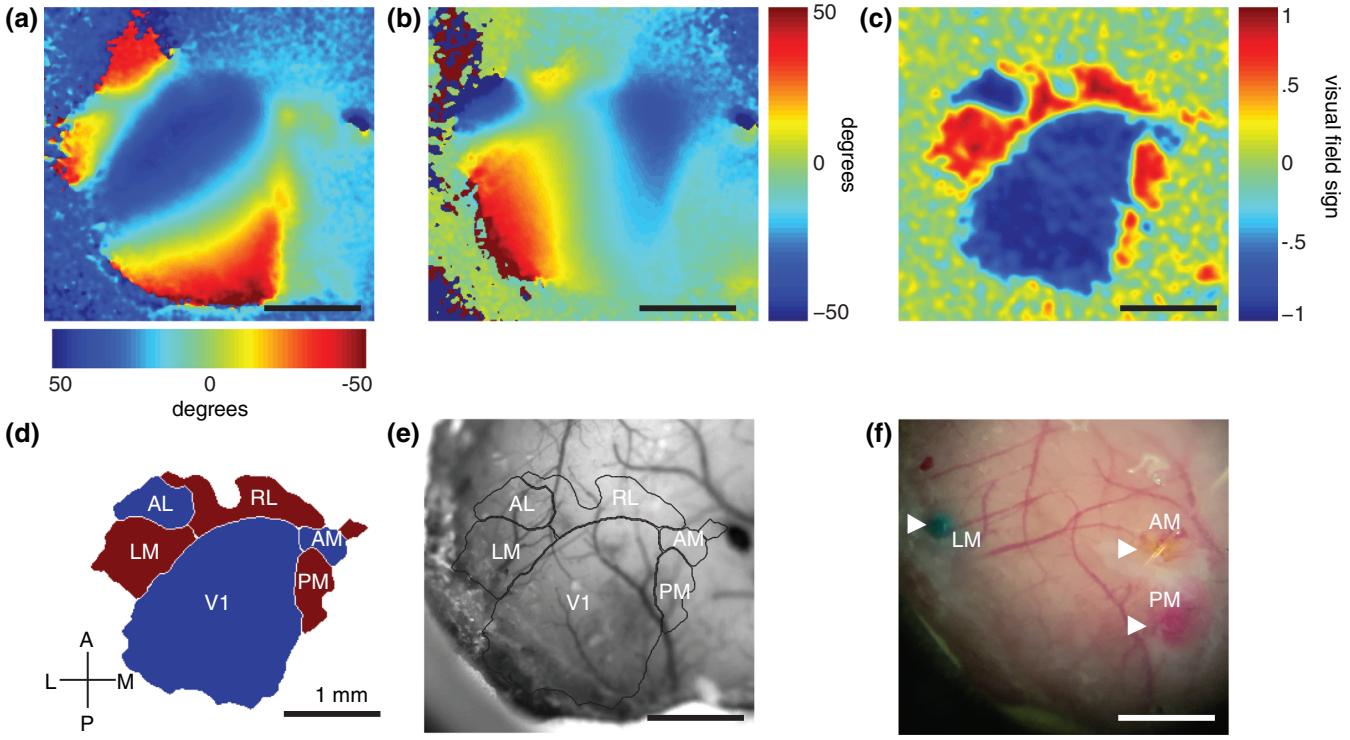

FIGURE 1 Identification of visual areas for AF-CTB injection. (a) Example azimuth retinotopic map. (b) Example altitude retinotopic map. (c) Visual field sign map, computed from the retinotopic maps in (a). (e) Outline of identified visual areas. Blue areas have a mirror representation of visual space, red areas have a nonmirror representation. It is often difficult to obtain retinotopic maps from P/POR, in the far posterolateral corner of the window—Often P/POR injections were guided by injecting posterior to LM and lateral to V1. (e) Visual area borders overlaid on the corresponding blood vessel image acquired with a green light over the intact skull. (f) Image through the skull taken shortly after AF-CTB injection (*white arrowheads*) into LM (647), AM (488), and PM (555). Even through the skull, blood vessels and AF-CTB spread are visible. All figures are from Animal 3–8 (Table 1). All scale bars are 500 μm [Color figure can be viewed at wileyonlinelibrary.com]

of AF for each injection was random and is well-balanced across animals (Table 1). Mice were anesthetized with 100 mg/kg of ketamine and 10 mg/kg xylazine cocktail via intra-peritoneal injections and mounted in a stereotax (David Kopf Instruments Model 940 series, Tujunga, CA) for surgery and stereotaxic injections. To expose the brain for injection, either a burr hole was drilled or a craniotomy was performed over visual cortex. Injections were done with air pressure using a picospritzer (General Valve Corp, Fairfield, NJ). To prevent backflow, the pipette was left in the brain for 5 min before and after injection.

AF-CTB was injected into visual cortical areas based on functional retinotopic maps overlaid on the blood vessel pattern, using these blood vessels as landmarks (Figure 1). When multiple areas were injected, the injections were targeted to matched retinotopic locations. AF-CTB pressure injections into cortex were 20–50 nL for AL, AM, PM, and P/POR, and 40–100 nL for V1, LM, and RL, with 20–40 PSI and a 20–30 μm diameter pipette (Conte, Kamishina, & Reep, 2009). These conditions were optimal in order to restrict CTB to <300 μm diameter injection sites, a necessary condition for small visual areas. After recovery, mice were given water with ibuprofen (Perrigo Oral Suspension, for dose of 30 mg/kg) and housed for 4–6 days before tissue harvesting.

TABLE 1 Overview of all animals injected, organized by animals with three, two, or one successful injection(s) of AF-CTB

Mouse ID	488	555	647
3-1	RL	V1	LM
3-2	RL	LM	V1
3-3	AL	LM	V1
3-4	AM	RL	LM
3-5	PM	RL	P/POR
3-6	P/POR	PM	V1
3-7	PM	P/POR	LM
3-8	AM	PM	LM
3-9	PM	LM	AL
2-1	V1	PM	-
2-2	RL	-	AL
2-3	PM	-	AL
1-1	-	-	AL
1-2	-	-	RL
1-3	-	-	AL
1-4	-	-	AM
1-5	-	-	AM
1-6	LM	-	-

2.3 | Histology

Brains were harvested after transcardial perfusion using phosphate-buffered saline (PBS) followed by 4% paraformaldehyde (PFA). Brains were dissected out from skulls and postfixed with 2% PFA and 15% sucrose in PBS at 4°C overnight, and then immersed in 30% sucrose in PBS at 4°C before sectioning. Using a freezing microtome, 50 μm coronal brain sections were cut and stored in PBS with 0.01% sodium azide at 4°C. Sections were mounted on slides with Polyvinyl alcohol mounting medium containing DABCO and allowed to air-dry.

2.4 | Image acquisition and processing

Each section was imaged at 10× using an Olympus BX63 Microscope with parameters adjusted based on the intensity of expression and background fluorescence. The injection sites for each animal were measured to ensure restriction to small cortical visual areas. For LM and RL injections, animals with injection site diameters greater than 500 μm for LM or RL were excluded. For AL, AM, PM, and P/POR, animals with injection site diameters greater than 300 μm were excluded.

To compute average expression patterns in LP (Figure 4B), sections at −1.9 and −2.3 AP for each animal were aligned to the Paxinos Mouse Atlas using the Landmark Correspondences macro in Fiji (Paxinos & Franklin, 2013; Schindelin et al., 2012; https://imagej.net/Landmark_Correspondences). Borders indicating the extent of expression in the thalamus were manually drawn for each animal and overlaid on the Paxinos and Franklin atlas outlines. Thalamic divisions and subcortical area borders were drawn manually, using the atlas and cell densities (as marked by DAPI) as a guide.

To determine the number of cells projecting to multiple visual areas, we imaged the sections with at least two different AF-CTB types of retrogradely labeled cells at 20× using a Zeiss LSM780 confocal microscope. For each brain with multiple successful AF-CTB injections, every fourth section was imaged (~200 μm apart, 4–10 sections per mouse) and all cells in zones of LP with multiple tracers were manually counted. Because almost all of the regions with intermingled cells were in LPMR (see Figures 2 and 5 for illustration), these counts largely reflect the cells in LPMR, and on the LPLR/LPMR border. Percentages reported are the number of cells double-labeled with two different tracers divided by sum of the numbers of cells labeled by each of the same two tracers in LP.

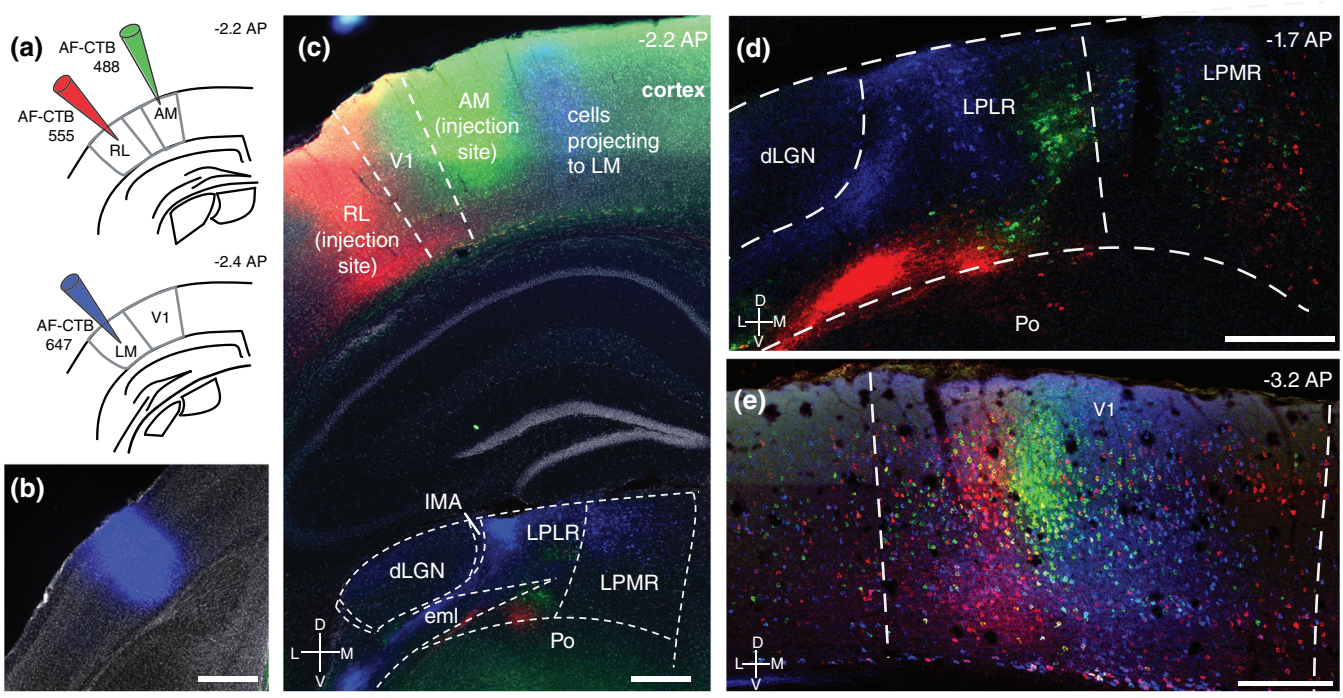

FIGURE 2 The injection of three different retrograde tracers into one mouse demonstrates robust label in the thalamus and overlapping label in V1. (a) Schematic of experiment. Three different colors of AF-CTB were injected into three different functionally-identified cortical areas. (b) Coronal brain section showing injection into LM (AF-CTB 647). (c) Coronal brain section showing injections into RL (red, AF-CTB 555) and AM (green, AF-CTB 488), as well as retrogradely labeled areas of the thalamus and cortex. (d) Confocal image of the thalamus, demonstrating nonoverlapping label in LPLR, and intermingled but nonoverlapping label in LPMR. (e) Confocal image of V1, demonstrating widespread retrograde label, with overlapping regions of cells (few of which are double-labeled). Abbreviations: AF-CTB, alexa fluor conjugated cholera toxin B; AM, anteromedial visual area; dLGN, dorsal lateral geniculate nucleus; eml, external medullary lamina; IMA, intramedullary thalamic area; LM, lateromedial visual area; LPLR, laterorostral lateral posterior nucleus; LPMR, mediorostral lateral posterior nucleus; Po, posterior thalamic nucleus; RL, rostrolateral visual area. Data from Animal 3–4. All scale bars are 500 μm [Color figure can be viewed at wileyonlinelibrary.com]

2.5 | Experimental design and statistical analysis

All mice used are detailed in Table 1. Mice used in this study (n = 19 total) were all C57BL/6, both male and female, and aged from 5 to 14 weeks. With seven different targeted visual areas, >3 injections per area in different mice ensures reliability of our results. For analysis of double-labeled cells, we sectioned each brain at 50 μm and counted cells in every fourth section (additional details about related methods can be found in Histology and Image acquisition and processing). Any computed statistic (i.e., percentages in Figures 5g,h and 6f) are explained in the figure legends. We did not conduct any statistical analyses in this article.

3 | RESULTS

We investigated the organization of thalamocortical projections by functionally mapping visual cortex and then injecting retrograde tracers into seven different visual areas. We mapped the retinotopic organization of the visual cortex in each mouse using intrinsic signal imaging (Figure 1a–c; Juavinett et al., 2017). Using these maps, we automatically constructed borders between visual areas (Figure 1d,e; Garrett et al., 2014). We then used simultaneously imaged surface blood vessel patterns to target injections of an efficient retrogradely-transported neuroanatomical tracer, Cholera Toxin Subunit B, conjugated to various Alexa fluorophores (Figure 1f; AF-CTB).

We injected 18 mice with various combinations of one, two, or three different AF-CTB tracers into seven different visual cortical areas, giving 39 total injections (Table 1). When multiple tracers were injected they were injected at retinotopically matched locations, as verified by overlapping label within V1 (see below). This approach allowed us to directly compare the thalamic zones that provide input to different cortical areas from retinotopically matched locations in the same mice. It also allowed quantification of the proportions of thalamic neurons that project to multiple visual cortical areas.

We were able to achieve robust, and reliable labeling patterns using AF-CTB. Figure 2 shows an example of an experiment in which three different colors of AF-CTB (488, 555, 647) were injected into three different visual cortical areas (AM, RL, LM, respectively) in the same mouse (Figure 2a–c). Each visual area received input from one or multiple patches in the thalamus (Figure 2c,d). In this example, LM, AM, and RL received input from separate patches in LPLR. LM predominately received input from the area of LPLR closest to the dLGN, while the more anterior cortical area RL received input from ventral LPLR, bordering on Po. AM received input from the medial part of LPLR. Each of these areas also received relatively weaker and more widespread input from LPMR (Figure 2d).

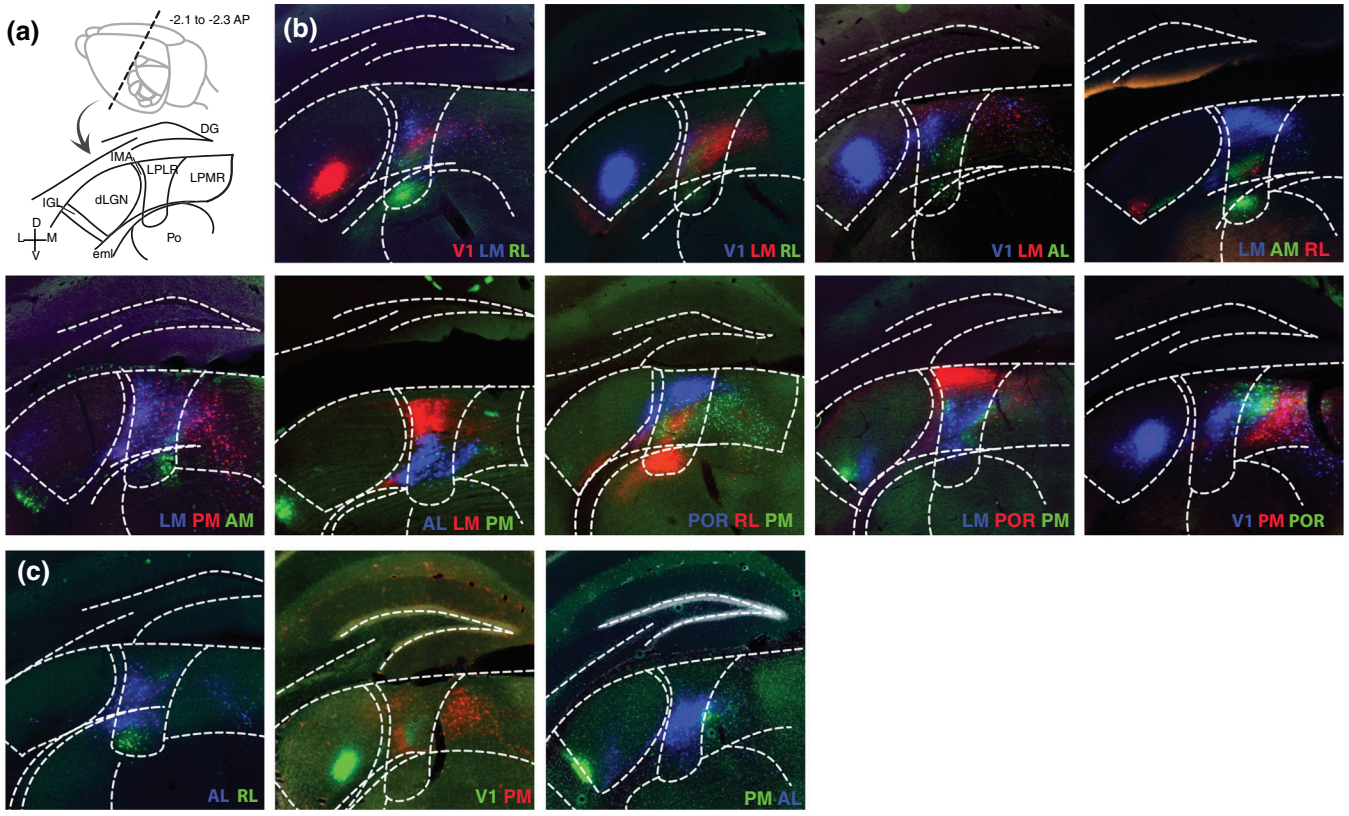

FIGURE 3 Brains with multiple injections demonstrate systematic organization of inputs from thalamus to visual cortical areas. (a) Schematic of experiment and atlas section (modified from Paxinos & Franklin, Bregma −2.3 mm). (b) Nine experiments with three injections of AF-CTB into each animal. (c) Additional experiments with two injections to further demonstrate relationships between projection regions for V1, RL, AL, and PM [Color figure can be viewed at wileyonlinelibrary.com]

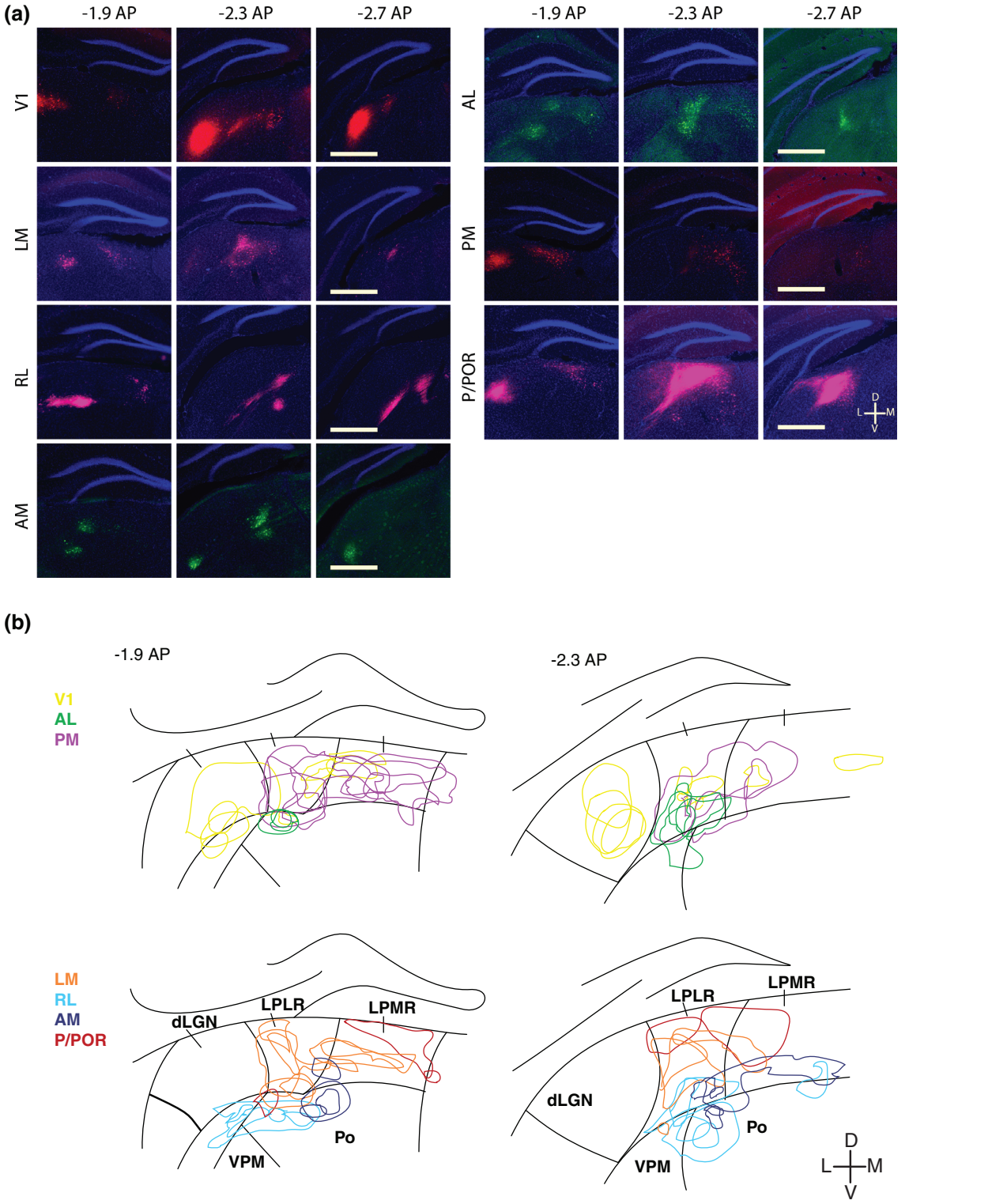

FIGURE 4 Single injection cases and alignment to common atlas. (a) Example labeling pattern of input into each visual area tested. Scale bar = 500 um. (b) By aligning each thalamic section to a common atlas (see Section 2), we can begin to see trends across animals [Color figure can be viewed at wileyonlinelibrary.com]

For mice with multiple injections, we confirmed the spatial overlap of cells in V1 to assure that the injection sites were in overlapping retinotopic locations (Figure 2e). Thus, any differences in the topographic locations of labeled thalamic neurons must be attributed primarily to differences related to the areas that the thalamic cells project to rather than retinotopy. Given the small size of extrastriate cortical areas and the retinotopic extent of label observed in V1, we are confident that each AF-CTB injection here covered a large portion

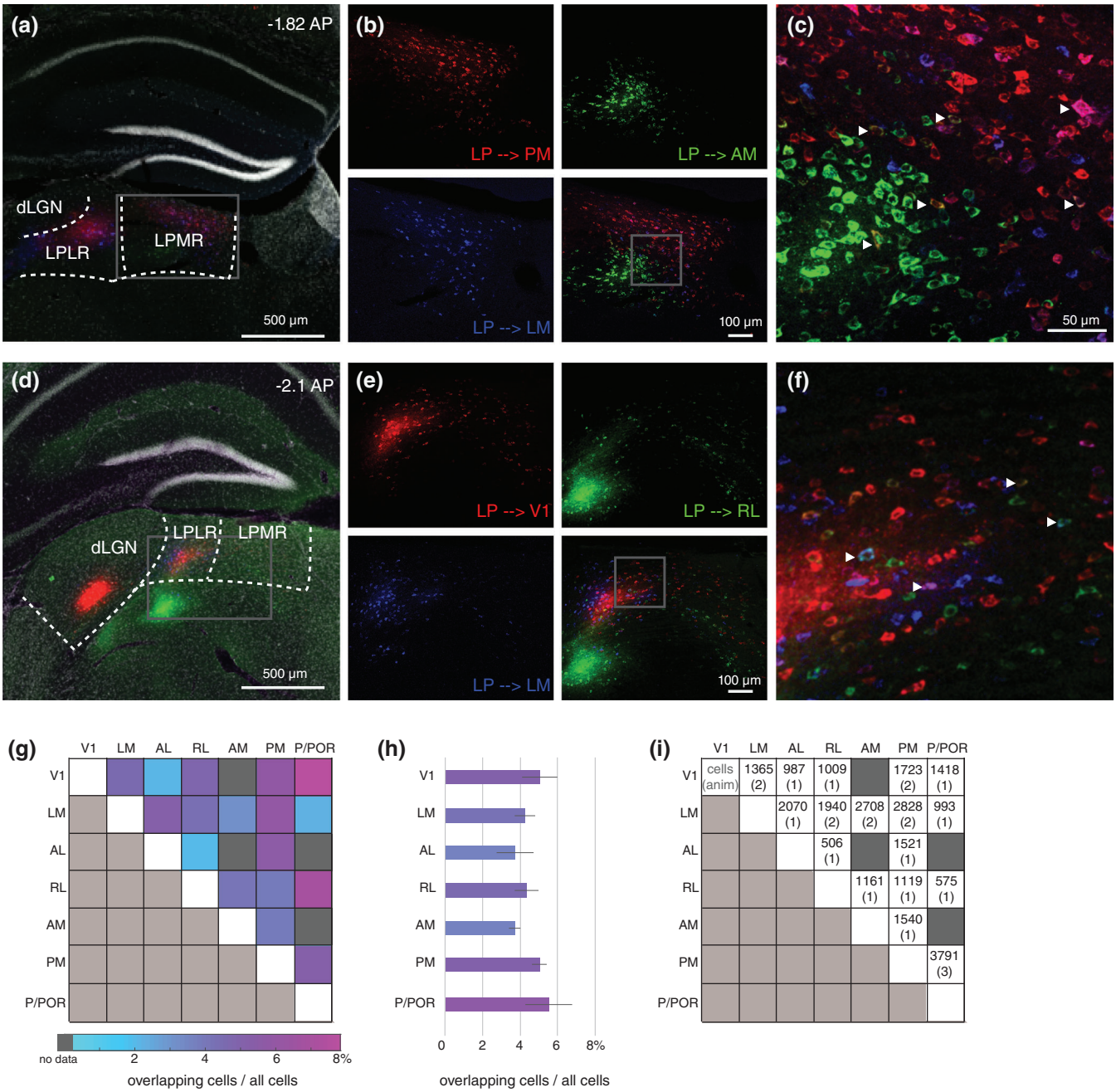

FIGURE 5 Percentages of LP cells projecting to multiple visual areas. (a) Overview of sample experiment (Animal 3–8) with three different tracer injections into PM, LM, and AM, demonstrating very little overlap of projection zones. (b) Low resolution image to demonstrate locations of cells projecting to PM, LM, and AM; field of view is marked by gray box in (a). (c) High resolution confocal images of LP showing cells projecting to PM, LM, and AM; field of view is marked by gray box in (b), white arrows point to rare double-labeled cells. (d) Sample experiment (Animal 3–1), demonstrating very little overlap of LP projections to V1, LM, and RL. (e) Low resolution image to demonstrate retrogradely labeled cells from V1, LM, and RL; field of view is marked by box in (e). (f) High resolution confocal images of LP showing cells projecting to V1, LM, and RL; field of few is marked by gray box in (e); white arrows point to rare double-labeled cells. (g) Quantification of cells that project to multiple visual areas. Percentages shown are # overlapping cells/total # cells in LP. Most combinations are based on a single animal and the following combinations included two animals: V1/LM, V1/PM, LM/RL, LM/AM, LM/PM. (h) Average percent overlap for each visual area with all other visual areas. Error bars are *SEM*. All measures of percentages of double-labeled cells are based on the total numbers of cells counted from either one or two animals that included the relevant combinations. (i) Total numbers of cell counts and animals (anim; in parentheses) for each visual area combination [Color figure can be viewed at wileyonlinelibrary.com]

of visual space. While labeled cells in V1 are found in both overlapping and nonoverlapping zones, as expected from the biases in visual field representations of the different extrastriate areas, the presence of overlap indicates that we successfully injected locations with overlapping retinotopic locations. Few cells in these overlapping V1 areas were double-labeled.

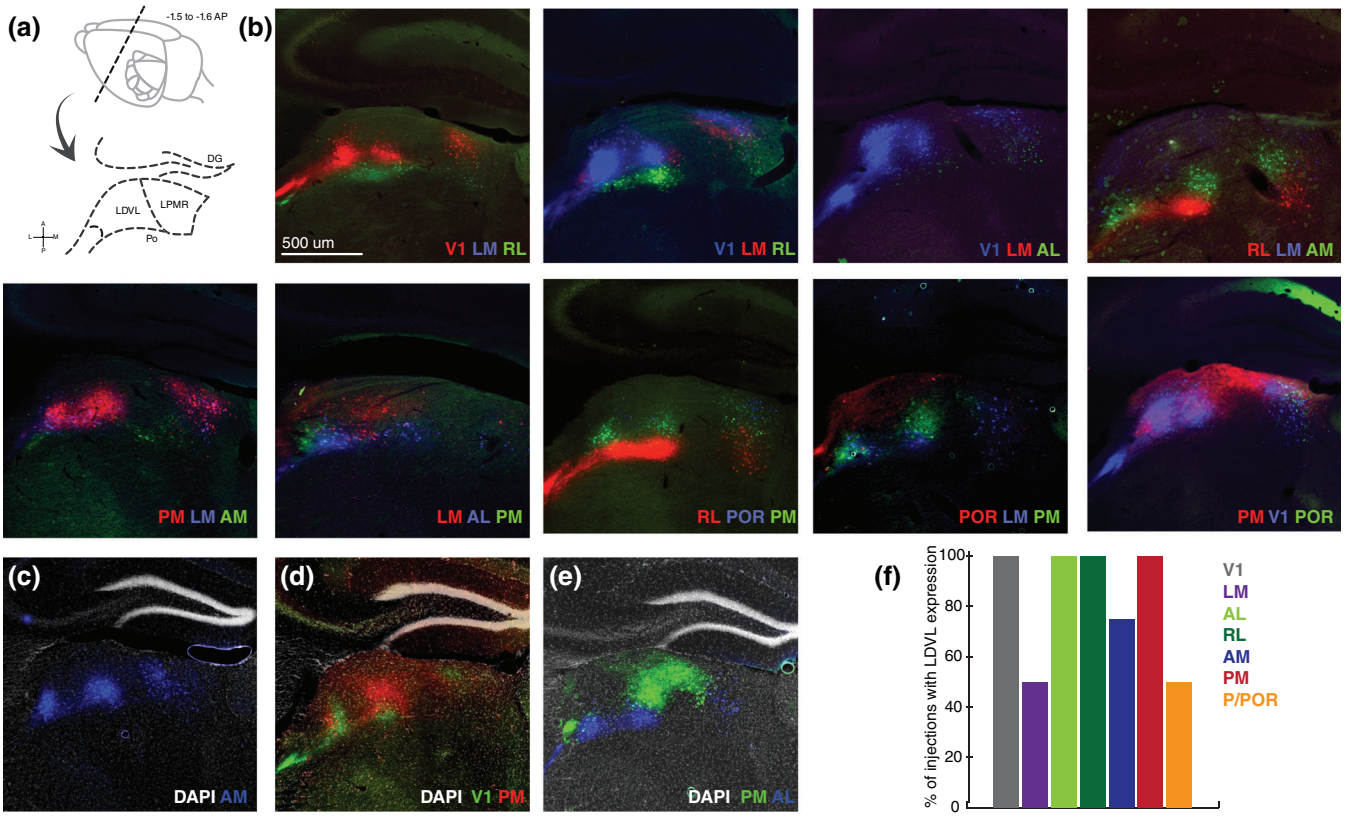

FIGURE 6 V1 and extrastriate cortical areas receive input from LDVL. (a) Schematic of brain section, modified from Paxinos & Franklin. (b) Triple injection brains demonstrating inputs from LDVL and LPMR. V1, RL, AM, and PM injections consistently result in substantial label in LDVL. LM, AL, and POR injections result in weaker and inconsistent label in LDVL. (c) Additional brain confirming LDVL projections to AM. (d) Additional brain demonstrating LDVL projections to V1 and PM. (e) Additional brain demonstrating LDVL projections to PM and AL. (f) Percent of brains with retrogradely labeled cells in LDVL for each injected cortical visual area [Color figure can be viewed at wileyonlinelibrary.com]

It is noteworthy that small differences in the V1 locations with the most dense retrograde label correspond to retinotopic distances that would predict only extremely small distances across the corresponding retinotopy in LP. For example, despite extensive overlap of AM-projecting (green) and RL-projecting (red) V1 neurons illustrated in Figure 2e, the locations of densest label are separated by about 200 μm along the medio-lateral axis. Retinotopic mapping of LP projections to V1 reveals that neurons separated by 1 mm mediolaterally in V1 receive input from LP neurons separated by only 100 μm (Roth et al., 2015). Thus, if the LP neurons projecting to AM versus RL in our Figure 2D were separated in position solely due to retinotopic differences in injection location, they should be separated by only about 20 μm. This is far less than the roughly 1 mm center-to-center spacing observed (Figure 2d), arguing that the different locations of LP neurons projecting to AM versus RL are not due to retinotopic mapping within LP.

Across the nine mice for which three successful cortical injections were made and three mice with two injections, we see similar patterns of retrograde labeling for each visual area (Figure 3). Within animals, we find that well-segregated zones of LP project to different visual areas for every combination of areas examined. Furthermore, there is a systematic relationship between LP projection zones and cortical areas that is conserved across animals (summarized schematically in Figure 7). As a general rule, the more posterior visual cortical areas receive input from more dorsal locations in LP, while more anterior cortical areas receive input from more ventral locations in LP. Across the mediolateral cortical axis, more lateral cortical areas receive input from more lateral LP and medial from medial. These trends are seen most clearly in the triple and double injection cases where, within each animal, the same topographic relationships are invariably observed (Figure 3) despite some variability between animals in the precise alignment to anatomical boundaries defined by the Paxinos and Franklin Atlas (Figure 4; Paxinos & Franklin, 2013).

For example, consider that the centers of the most lateral visual areas (including V1), progressing from posterior to anterior are P/POR, LM, V1, AL, and RL. Label within LP from P/POR injections (Figure 3 Panels B7–B9) is located dorsal to label from injections in LM (B8), V1 (B9), and RL (B7). Similarly, LP label from LM injections is consistently more dorsal than that from injections in all other areas (except P/POR) and most notably is consistently just slightly more dorsal than LP label from V1 injections (Figure 3, Panels B1, B3). Injections in the next most anterior cortical area, AL, yield LP label that is more ventral than from injections in LM (B3, B6) or V1 (B3), but more dorsal than label from an injection in RL. Injections in RL consistently

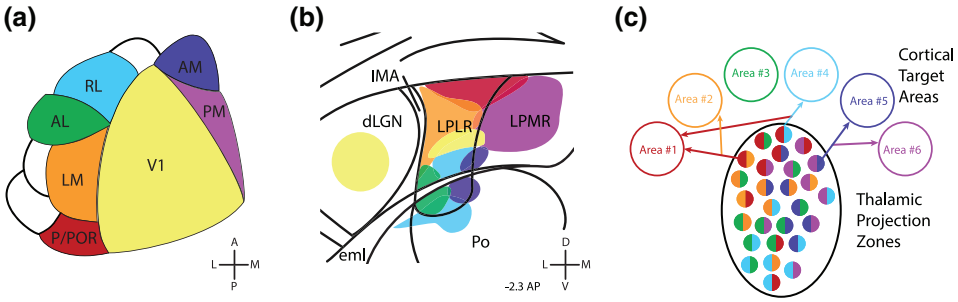

FIGURE 7 Overview schematic demonstrating corresponding topographic mapping between visual cortex and LP. (a) The visual cortex of the mouse; areas investigated in the present study are colored. (b) Schematic of projection zones in the mouse thalamus colored according to the cortical area to which they project. The thalamic organization is flipped relative to cortex, with anterior visual cortex represented in the ventral thalamus, while posterior visual cortex is represented in the dorsal thalamus. Lateral and medial organization is conserved. It should be noted that this schematic reflects most of, but not all, projections. Retrograde label was seen in LP beyond the borders denoted here. This schematic is meant to reflect the bulk of these cells and is based on the maximum intensity of the retrograde label (see Figure 4b and Section 2). (c) Given the systematic differences in the locations of LP cells projecting to different cortical areas, our low observed proportions of double retrograde labeling, and previous reports of cells in LP with projections to 2–3 locations, we suggest a scheme in which many cells in LP project to multiple cortical areas. However, due to the many possible combinations of visual areas, few cells are double-labeled by any particular combination. In this schematic example, each LP neuron projects to just two areas, as indicated by the color coding for each cell. Most cells projecting to a particular location are grouped together but they also have a secondary projection to one of the other areas [Color figure can be viewed at wileyonlinelibrary.com]

result in the most ventral LP label (B1, B2, C1), most notably in a direct comparison, more ventral than label following injection in AL (C1).

On the medial side of V1, cortical injections were made into areas AM and PM. LP label following injections in area PM was consistently located more medially than label from injections in any other cortical area (see Figure 3, Panels B5–6, C2–3). Furthermore, when AM and PM were both injected in the same animal (B5), label in AM is located more ventrally and laterally, consistent with the general trend for more anterior areas to receive more ventral LP input and for more medial cortical areas to receive more medial LP input. (This medial-lateral relationship is most pronounced if we consider a skewed "AP-axis" extending along the representation of the vertical meridian at the lateral edge of V1.)

Despite the clear and consistent within-animal relationships between LP projection zones and recipient cortical areas, there is scatter in the positions of LP cell clusters from same area injections aligned to the Atlas across different animals. Thus, when single injection cases are aligned to the atlas (Figure 4B) the general overall topographic trends can be observed but they are not as clear. Similar between-animal trends are also seen in the multi-injection cases (Figure 3). This variability might reflect true biological variability, such as the inability of a single idealized atlas to accurately map to animals with differences in brain structure, or systematic between animal shifts in the topographic locations of LP cells projecting to each cortical area. Alternatively, these differences might reflect experimental variability such as the plane of brain sectioning or choice of alignment between finely spaced brain sections (50 μm) and more intermittent sampling in the atlas (120 μm). Despite scatter between cases and resulting overlap in projection zones for thalamic neurons projecting to some visual areas, there was still clear segregation between LM and PM projecting neurons, with PM projecting neurons located in very anterior/medial LP, and LM projecting neurons in lateral/posterior LP. RL, AM, and AL all had two patches of input in the thalamus, divided by the external medullary lamina (eml), perhaps reflecting dual retinotopic maps within LP (Bennett et al., 2019).

While there were clear trends in the relative topographic locations of LP neurons projecting to different cortical areas, there was also clear intermingling of cells (Figures 2–4), particularly for cases involving multiple injections into neighboring cortical areas. Do these thalamic neurons nevertheless represent dedicated projection channels or do some cells project to more than one cortical area? We further analyzed cases with 2 to 3 different AF-CTBs into each mouse, to quantify the percent of overlap between projections to different visual areas (Figure 5). For this purpose, we analyzed sections with overlap between retrogradely labeled areas. There were very few cells that were double-labeled (~3–6% of all retrogradely labeled cells in LP; Figure 5g,h). Across the other visual areas, P/POR had the highest overlap (5.5%), followed by PM and V1 (5.0%). The weakest overlap was between AL and RL, with only 2.0% of all cells double-labeled. The strongest overlap was between V1 and P/POR, with 7.8% of cells double-labeled. Only zones with overlapping cells were counted in order to rule out the possibility that a lack of dual projections could be due to differences in retinotopic locations of injection in different cortical areas. Insofar as there is retinotopy in the thalamus, the quantified neurons must be from matched retinotopic locations where the cortical injections had overlapping retinotopy.

In addition, the ventrolateral part of the laterodorsal nucleus (LDVL) had significant retrograde label from extrastriate areas. Injections in V1, AL, RL, and PM consistently resulted in label in LDVL (Figure 6). LM, AM, and P/POR had inconsistent label in LDVL: 4 of 8 LM injections, 3 of 4 AM injections, and 2 of 4 P/POR injections

had visible label in LDVL. In all cases in which label was visible in LDVL, close inspection across multiple brain sections revealed that the group of labeled neurons was clearly separated from and not contiguous with the label in LP. We did not see label in the dorsomedial part of the laterodorsal nucleus (LDDM) in any mouse.

4 | DISCUSSION

Using classic tracing techniques combined with intrinsic signal imaging, here we show that the mouse lateral posterior nucleus (LP) is topographically organized, with neurons projecting to different visual areas being located predominantly in different locations. This organization is orthogonal to retinotopic mapping within LP. Furthermore, the ventrolateral part of the laterodorsal thalamic nucleus (LDVL) projects to multiple visual cortical areas. As a comprehensive look at the organization of this underappreciated nucleus, this study lays important groundwork for future investigations into LP function in mice and provides a framework to test theories of thalamocortical circuit organization.

Extrastriate areas in the mouse are known to have biases in retinotopic field coverage (Garrett et al., 2014; Zhuang et al., 2017). We designed experiments to independently assess whether there might be a clear topography of LP projections, in addition to the known retinotopy. We find that in addition to the retinotopic maps along the A-P and M-L axes of LP (Bennett et al., 2019; Roth et al., 2015), neurons projecting to the more anterior visual areas (e.g., RL) are located more ventrally than those projecting to more posterior visual areas (e.g., P/POR; Figure 7). These patterns cannot be explained by retinotopy within LP, because they occur on a much larger spatial scale: previous studies of LP inputs to different locations within mouse V1 show that there is retinotopy *within* a 500 μm zone of LP (Roth et al., 2015) whereas our projection zones are often more than 500 μm apart. V1 injections that were 500 μm apart resulted in ~100 μm spread of LP label, suggesting a fivefold compression of the map in LP relative to V1 (Roth et al., 2015). It should also be noted that a topographic organization similar to what we observe in mice has also been observed in nonhuman primates (Baldwin et al., 2017; Kaas & Lyon, 2007; Shipp, 2001, 2003; Stepniewska, Qi, & Kaas, 1999). We speculate that this is a common feature of connections between pulvinar and cortex and would be observed in all species if suitable methods were employed. It is likely to be more readily apparent from comparisons of single injections into different animals in primates, where pulvinar is typically much larger than in rodents. The use of retinotopic cortical mapping and retinotopically matched injections into multiple cortical areas is likely to facilitate these observations in animals with smaller brains, as we have demonstrated here.

Analyses of retrograde labeling following tracer injections into two or three visual areas revealed few double labeled cells, indicating that most cells do not project to the particular combinations of areas that were injected. Taken at face value, this could be interpreted to indicate that few cells project to multiple areas. But reconstructions of single thalamic neurons reveal a range of anatomical cell types including some that have very focused cortical projections and others with more widespread projections (Clascá, Rubio-Garrido, & Jabaudon, 2012). An alternative scenario, suggested by these observations and by limited single cell reconstructions in mice (Nakamura et al., 2015; Janelia MouseLight Project) would be that LP cells project to more than one cortical region but to only a very limited subset of visual cortical areas. Or cells might project to just one of the visual areas that we sampled plus an additional area, such as the restrosplenial cortex, which we did not inject. For example, suppose that all of the LP neurons located in a particular topographic zone have a high probability of projecting to a corresponding cortical location and additionally project to just one of nine or more other possible cortical targets (Figure 7c). With such an organization, there would be very few double labeled cells resulting from any combination of two retrograde tracer injection locations, as we have observed, but single cell reconstructions would reveal multiple projections from single neurons (Nakamura et al., 2015; Janelia MouseLight Project; http://ml-neuronbrowser.janelia.org). A similar organization has been demonstrated for cortico-cortical projections of mouse V1 neurons (Han et al., 2018). In view of our observation that neurons in different topographic locations within LP have very strong biases in the visual cortical areas to which they project, we favor this interpretation.

Understanding the anatomy of thalamocortical projections can lend criticism or credit to various theories about thalamocortical function. A common label for LP/pulvinar is that of a “gate” or “router” for information as it travels through cortex, perhaps for the purposes of synchronization or multisensory processing (Ahissar & Oram, 2013; Cappe, Morel, Barone, & Rouiller, 2009; Crick & Koch, 1998; Olshausen et al., 1993; Shipp, 2003). If single neurons in LP acted to synchronize disparate areas of cortex, we would expect them to project to multiple regions. Other theories of thalamic function require more precise anatomical channels, for instance to selectively route information through the cortical hierarchy (Sherman & Guillery, 2002). If LP is a router for information up the visual hierarchy, single cells in LP should receive input from cortical areas and specifically route them to higher-order areas. While our data provide new information that would constrain the precise way that these functions are implemented, they do not exclude or validate any of these hypotheses. As described above, we favor the interpretation that these circuits do not fit into either extreme model but instead have aspects that would allow them to flexibly facilitate both interactions across cortical areas and more directed routing of information.

In primate thalamus, there are two different sets of thalamocortical connections: cells in the “core” which express parvalbumin and project to specific areas of cortex, and cells in the “matrix,” which express calbindin and project broadly to superficial cortex (Jones, 1998). These two projection types, one targeted and one broad, could enable different modes of thalamic functioning, to synchronize vast areas of cortex and/or specifically route information (Jones, 1998, 2001). While we cannot distinguish between these core and matrix populations with our methods, the small proportion of double-labeled cells in our data suggests that the thalamus is poised to perform both functions––a limited number of cells may send

broader information, while other cells may specifically project to only one or to a more limited set of other cortical regions. It is possible that the majority of double-labeled cells that we observed are matrix cells, but additional experiments would be needed to confirm this hypothesis.

This distinction between core and matrix pathways may be the necessary anatomical substrate for setting necessary bounds on corticothalamocortical loops, also known as "the no-strong-loops" hypothesis. This framework posits that no two brain areas can have reciprocal excitatory, driving connections (Crick & Koch, 1998). LP inputs and outputs are segregated between layers of cortex, with the exception of possible overlap in Layer 5 (L5): LP receives input from L5 of cortex, a putative driving connection (Bourassa & Deschênes, 1995; Kim, Juavinett, Kyubwa, Jacobs, & Callaway, 2015), and projects to L5 and L6 of V1 and L4, L5, and L6 of extrastriate cortex (Roth et al., 2015). According to the no-strong-loops hypothesis, LP cells receiving this driving cortical input from L5 should not project back to L5 of the same cortical region. Several visual areas, including RL, AL, and AM, receive input from two separate patches in LP. It is possible that these are separate sets of cells that receive driving versus modulatory input, that in return project to different layers or cortical areas, however, this needs to be directly tested. It is also possible that these patches are actually one functional group of cells that is anatomically split by the external medullary lamina.

Furthermore, our study provides the first published evidence that the ventral part of the laterodorsal nucleus (LDVL) provides significant input to V1, AL, RL, AM, and PM, and perhaps also LM and P/POR. LDVL is known to project to cingulate, retrosplenial, and posterior parietal cortex (Jones & Leavitt, 1974; Robertson, 1977; Spiro, Massopust, & Young, 1980). With such diffuse inputs and outputs, there is wide speculation on the functional role of LD (Bezdudnaya & Keller, 2008). Previous anatomical reports combined with our data suggest that there is a path from visual cortex through LDVL to various limbic and associative areas (Jones & Leavitt, 1974; Robertson & Kaitz, 1981). This pathway may be important for the inclusion of visual input in spatial, emotional, or decision-making behavior (Poort et al., 2015).

A critical question remains: what are the inputs to cells in LP or LDVL with projections to different visual cortical areas? Connecting our observations here to previous studies of the input zones of LP can inform our expectations based on the spatial overlap of inputs and outputs (Zhou, Maire, Masterson, & Bickford, 2017). In cats, LPLR receives input from V1, while LPMR receives input from SC (Chalupa & Abramson, 1989). In rats, the distinction between V1 and SC recipient regions lies along the rostral-caudal axis: rostral LP receives cortical input, whereas caudal LP receives tectal input (Li, Wang, & Bickford, 2003). A recent study in mice suggests that LPLR receives input from one class of SC cells (Gale & Murphy, 2014), although there is other evidence that LPMR also receives input from SC (Allen Brain Institute Connectivity Atlas) as well as retinal ganglion cells (Allen et al., 2016). Future experiments utilizing retrograde viruses along with conditional transynaptic tracing viruses (Luo, Callaway, & Svoboda, 2018) will hopefully provide satisfying answers to these questions.

ACKNOWLEDGMENTS

This work was supported by the NIH grants EY022577, EY019005, and MH063912 and the Gatsby Charitable Foundation (E.M.C.). A.L.J. was supported by the National Science Foundation and Martinet Foundation.

CONFLICT OF INTEREST

The authors declare no competing financial interest.

ORCID

Edward M. Callaway https://orcid.org/0000-0002-6366-5267

REFERENCES

Abramson, B. P., & Chalupa, L. M. (1988). Multiple pathways from the superior colliculus to the extrageniculate visual thalamus of the cat. *The Journal of Comparative Neurology*, *271*, 397–418 Retrieved from http://www.ncbi.nlm.nih.gov/entrez/query.fcgi?cmd=Retrieve&db=PubMed&dopt=Citation&list_uids=2454967

Ahissar, E., & Oram, T. (2013). Thalamic relay or Cortico-thalamic processing? Old question, new answers. *Cereb Cortex*. Retrieved from http://www.cercor.oxfordjournals.org/cgi/doi/10.1093/cercor/bht296, *25*, 845–848.

Allen, A. E., Procyk, C. A., Howarth, M., Walmsley, L., & Brown, T. M. (2016). Visual input to the mouse lateral posterior and posterior thalamic nuclei: Photoreceptive origins and retinotopic order. *The Journal of Physiology*, *594*, 1911–1929 Retrieved from http://doi.wiley.com/10.1113/JP271707

Baldwin, M. K. L., Balaram, P., & Kaas, J. H. (2017). The evolution and functions of nuclei of the visual pulvinar in primates. *The Journal of Comparative Neurology*, *525*, 3207–3226 Retrieved from http://doi.wiley.com/10.1002/cne.24272

Baldwin, M. K. L., Wong, P., Reed, J. L., & Kaas, J. H. (2011). Superior colliculus connections with visual thalamus in gray squirrels (*Sciurus carolinensis*): Evidence for four subdivisions within the pulvinar complex. *The Journal of Comparative Neurology*, *519*, 1071–1094 Retrieved from http://doi.wiley.com/10.1002/cne.22552

Bennett, C., Gale, S. D., Garrett, M. E., Newton, M. L., Callaway, E. M., Murphy, G. J., & Olsen, S. R. (2019). Higher-order thalamic Circuits Channel parallel streams of visual information in mice. *Neuron*, *102*, 477–492.e5 Retrieved from https://linkinghub.elsevier.com/retrieve/pii/S0896627319301199

Bezdudnaya, T., & Keller, A. (2008). Laterodorsal nucleus of the thalamus: A processor of somatosensory inputs. *The Journal of Comparative Neurology*, *507*, 1979–1989 Retrieved from http://doi.wiley.com/10.1002/cne.21664

Bourassa, J., & Deschênes, M. (1995). Corticothalamic projections from the primary visual cortex in rats: A single fiber study using biocytin as an anterograde tracer. *Neuroscience*, *66*, 253–263.

Cappe, C., Morel, A., Barone, P., & Rouiller, E. M. (2009). The thalamocortical projection systems in primate: An anatomical support for multisensory and sensorimotor interplay. *Cerebral Cortex*, *19*, 2025–2037.

Chalupa, L. M., & Abramson, B. P. (1989). Visual receptive fields in the striate-recipient zone of the lateral posterior-pulvinar complex. *The Journal of Neuroscience*, *9*, 347–357 Retrieved from http://eutils.ncbi.nlm.nih.gov/entrez/eutils/elink.fcgi?dbfrom=pubmed&id=2913211&retmode=ref&cmd=prlinks

Clascá, F., Rubio-Garrido, P., & Jabaudon, D. (2012). Unveiling the diversity of thalamocortical neuron subtypes. *The European Journal of Neuroscience*, *35*, 1524–1532 Retrieved from http://doi.wiley.com/10.1111/j.1460-9568.2012.08033.x

Conte, W. L., Kamishina, H., Corwin, J. V., & Reep, R. L. (2008). Topography in the projections of lateral posterior thalamus with cingulate and medial agranular cortex in relation to circuitry for directed attention and neglect. *Brain Research*, *1240*, 87–95 Retrieved from https://doi.org/10.1016/j.brainres.2008.09.013

Conte, W. L., Kamishina, H., & Reep, R. L. (2009). Multiple neuroanatomical tract-tracing using fluorescent Alexa Fluor conjugates of cholera toxin subunit B in rats. *Nature Protocols*, *4*, 1157–1166 Retrieved from http://www.nature.com/doifinder/10.1038/nprot.2009.93

Crick, F., & Koch, C. (1998). Constraints on cortical and thalamic projections: The no-strong-loops hypothesis. *Nature*, *391*, 245–250 Retrieved from http://www.nature.com/doifinder/10.1038/34584

Felleman, D. J., & Van Essen, D. C. (1991). Distributed hierarchical processing in the primate cerebral cortex. *Cerebral Cortex*, *1*, 1–47 Retrieved from http://eutils.ncbi.nlm.nih.gov/entrez/eutils/elink.fcgi?dbfrom=pubmed&id=1822724&retmode=ref&cmd=prlinks

Gale, S. D., & Murphy, G. J. (2014). Distinct representation and distribution of visual information by specific cell types in mouse superficial superior colliculus. *The Journal of Neuroscience*, *34*, 13458–13471 Retrieved from http://www.jneurosci.org/cgi/doi/10.1523/JNEUROSCI.2768-14.2014

Garrett, M. E., Nauhaus, I., Marshel, J. H., & Callaway, E. M. (2014). Topography and areal organization of mouse visual cortex. *The Journal of Neuroscience*, *34*, 12587–12600 Retrieved from http://www.jneurosci.org/cgi/doi/10.1523/JNEUROSCI.1124-14.2014

Grieve, K. L., Acuña, C., & Cudeiro, J. (2000). The primate pulvinar nuclei: Vision and action. *Trends in Neurosciences*, *23*, 35–39 Retrieved from http://eutils.ncbi.nlm.nih.gov/entrez/eutils/elink.fcgi?dbfrom=pubmed&id=10631787&retmode=ref&cmd=prlinks

Han, Y., Kebschull, J. M., Campbell, R. A. A., Cowan, D., Imhof, F., Zador, A. M., & Mrsic-Flogel, T. D. (2018). The logic of single-cell projections from visual cortex. *Nature*, *556*, 51–56 Retrieved from http://www.nature.com/articles/nature26159

Jones, E. (1998). Viewpoint: The core and matrix of thalamic organization. *Neuroscience*, *85*, 331–345 Retrieved from https://www.sciencedirect.com/science/article/pii/S0306452297005812?via%3Dihub

Jones, E. G. (1985). *The thalamus*. New York, NY: Springer Science+Business Media.

Jones, E. G. (2001). The thalamic matrix and thalamocortical synchrony. *Trends in Neurosciences*, *24*, 595–601 Retrieved from https://www.sciencedirect.com/science/article/pii/S0166223600019226?via%3Dihub

Jones, E. G., & Leavitt, R. Y. (1974). Retrograde axonal transport and the demonstration of non-specific projections to the cerebral cortex and striatum from thalamic intralaminar nuclei in the rat, cat and monkey. *The Journal of Comparative Neurology*, *154*, 349–377 Retrieved from http://doi.wiley.com/10.1002/cne.901540402

Juavinett, A. L., Nauhaus, I., Garrett, M. E., & Callaway, E. M. (2017). Automated identification of mouse visual areas with intrinsic signal imaging. *Nature Protocols*, *12*, 32–43 Retrieved from http://www.nature.com/doifinder/10.1038/nprot.2016.158

Kaas, J. H., & Lyon, D. C. (2007). Pulvinar contributions to the dorsal and ventral streams of visual processing in primates. *Brain Research Reviews*, *55*, 285–296 Retrieved from http://linkinghub.elsevier.com/retrieve/pii/S0165017307000331

Kamishina, H., Conte, W. L., Patel, S. S., Tai, R. J., Corwin, J. V., & Reep, R. L. (2009). Cortical connections of the rat lateral posterior thalamic nucleus. *Brain Research*, *1264*, 39–56.

Kamishina, H., Yurcisin, G. H., Corwin, J. V., & Reep, R. L. (2008). Striatal projections from the rat lateral posterior thalamic nucleus. *Brain Research*, *1204*, 24–39 Retrieved from http://linkinghub.elsevier.com/retrieve/pii/S0006899308002291

Kim, E. J., Juavinett, A. L., Kyubwa, E. M., Jacobs, M. W., & Callaway, E. M. (2015). Three types of cortical layer 5 neurons that differ in brain-wide connectivity and function. *Neuron*. Retrieved from http://www.scopus.com/inward/record.url?eid=2-s2.0-84961653942&partnerID=MN8TOARS, *88*, 1253–1267.

Le Gros Clark, W. E. (1932). The structure and connections of the thalamus. *Brain*, *55*, 406–470.

Lent, R. (1982). The organization of subcortical projections of the hamster's visual cortex. *The Journal of Comparative Neurology*, *206*, 227–242 Retrieved from http://www.ncbi.nlm.nih.gov/pubmed/7085930

Li, J., Wang, S., & Bickford, M. E. (2003). Comparison of the ultrastructure of cortical and retinal terminals in the rat dorsal lateral geniculate and lateral posterior nuclei. *The Journal of Comparative Neurology*, *460*, 394–409 Retrieved from http://doi.wiley.com/10.1002/cne.10646

Luo, L., Callaway, E. M., & Svoboda, K. (2018). Genetic dissection of neural circuits: A decade of Progress. *Neuron*, *98*, 256–281 Retrieved from http://www.ncbi.nlm.nih.gov/pubmed/29673479

Marshel, J. H., Garrett, M. E., Nauhaus, I., & Callaway, E. M. (2011). Functional specialization of seven mouse visual cortical areas. *Neuron*, *72*, 1040–1054 Retrieved from https://doi.org/10.1016/j.neuron.2011.12.004

Mason, R. (1978). Functional organization in the cat's pulvinar complex. *Experimental Brain Research*, *31*, 51–66 Retrieved from http://eutils.ncbi.nlm.nih.gov/entrez/eutils/elink.fcgi?dbfrom=pubmed&id=639910&retmode=ref&cmd=prlinks

Nakamura, H., Hioki, H., Furuta, T., & Kaneko, T. (2015). Different cortical projections from three subdivisions of the rat lateral posterior thalamic nucleus: A single-neuron tracing study with viral vectors. *The European Journal of Neuroscience*, *41*, 1294–1310.

Nassi, J. J., & Callaway, E. M. (2009). Parallel processing strategies of the primate visual system. *Nature Reviews. Neuroscience*, *10*, 360–372.

Olshausen, B. A., Anderson, C. H., & Van Essen, D. C. (1993). A neurobiological model of visual attention and invariant pattern recognition based on dynamic routing of information. *The Journal of Neuroscience*, *13*, 4700–4719 Retrieved from http://eutils.ncbi.nlm.nih.gov/entrez/eutils/elink.fcgi?dbfrom=pubmed&id=8229193&retmode=ref&cmd=prlinks

Paxinos, G., & Franklin, K. B. J. (2013). *The mouse brain in stereotaxic coordinates* (2nd ed.). San Diego: Academic Press.

Poort, J., Khan, A. G., Pachitariu, M., Nemri, A., Orsolic, I., Krupic, J., … Hofer, S. B. (2015). Learning enhances sensory and multiple non-sensory representations in primary visual cortex. *Neuron*, *86*, 1478–1490 Retrieved from https://doi.org/10.1016/j.neuron.2015.05.037

Raczkowski, D., & Rosenquist, A. C. (1983). Connections of the multiple visual cortical areas with the lateral-posterior PULVINAR complex and adjacent thalamic nuclei in the cat. *The Journal of Neuroscience*, *3*, 1912–1942 Retrieved from papers3://publication/uuid/1846D787-C644-4DAA-9FAC-71B3CD1B5D31

Reep, R. L., & Corwin, J. V. (2009). Posterior parietal cortex as part of a neural network for directed attention in rats. *Neurobiology of Learning and Memory*, *91*, 104–113.

Robertson, R. T. (1977). Thalamic projections to parietal cortex. *Brain, Behavior and Evolution*, *14*, 161–184 Retrieved from http://www.ncbi.nlm.nih.gov/pubmed/851845

Robertson, R. T., & Kaitz, S. S. (1981). Thalamic connections with limbic cortex. I. Thalamocortical projections. *The Journal of Comparative*

Neurology, *195*, 501–525 Retrieved from http://doi.wiley.com/10.1002/cne.901950308

Robinson, D. L., & Petersen, S. E. (1992). The pulvinar and visual salience. *Trends in Neurosciences*, *15*, 127–132 Retrieved from http://eutils.ncbi.nlm.nih.gov/entrez/eutils/elink.fcgi?dbfrom=pubmed&id=1374970&retmode=ref&cmd=prlinks

Roth, M. M., Dahmen, J. C., Muir, D. R., Imhof, F., Martini, F. J., & Hofer, S. B. (2015). Thalamic nuclei convey diverse contextual information to layer 1 of visual cortex. *Nature Neuroscience*, *19*, 299–307 Retrieved from http://www.nature.com/doifinder/10.1038/nn.4197

Saalmann, Y. B., & Kastner, S. (2011). Cognitive and perceptual functions of the visual thalamus. *Neuron*, *71*, 209–223 Retrieved from http://linkinghub.elsevier.com/retrieve/pii/S0896627311005575

Schindelin, J., Arganda-Carreras, I., Frise, E., Kaynig, V., Longair, M., Pietzsch, T., … Cardona, A. (2012). Fiji: An open-source platform for biological-image analysis. *Nature Methods*, *9*, 676–682.

Sereno, M. I., Mcdonald, C. T., & Allman, J. M. (1994). Analysis of retinotopic maps in extrastriate cortex. *Cerebral Cortex*, *95*, 7121–7126.

Sherman, S. M., & Guillery, R. W. (1998). On the actions that one nerve cell can have on another: Distinguishing "drivers" from "modulators". *Proceedings of the National Academy of Sciences of the United States of America*, *95*, 7121–7126 Retrieved from http://www.pnas.org/content/95/12/7121.full

Sherman, S. M., & Guillery, R. W. (2002). The role of the thalamus in the flow of information to the cortex. *Philosophical Transactions of the Royal Society of London. Series B, Biological Sciences*, *357*, 1695–1708 Retrieved from http://rstb.royalsocietypublishing.org/cgi/doi/10.1098/rstb.2002.1161

Shipp, S. (2001). Corticopulvinar connections of areas V5 , V4 , and V3 in the macaque monkey : A dual model of retinal and cortical topographies. *The Journal of Comparative Neurology*, *490*, 469–490.

Shipp, S. (2003). The functional logic of cortico-pulvinar connections. *Philosophical Transactions of the Royal Society of London. Series B, Biological Sciences*, *358*, 1605–1624 Retrieved from http://rstb.royalsocietypublishing.org/cgi/doi/10.1098/rstb.2002.1213

Spiro, T., Massopust, L. C., & Young, P. A. (1980). Efferent projections of the lateral dorsal nucleus in the rat. *Experimental Neurology*, *68*, 171–184 Retrieved from http://www.ncbi.nlm.nih.gov/pubmed/7363984

Stepniewska, I., Qi, H. X., & Kaas, J. H. (1999). Do superior colliculus projection zones in the inferior pulvinar project to MT in primates? *The European Journal of Neuroscience*, *11*, 469–480 Retrieved from http://www.ncbi.nlm.nih.gov/pubmed/10051748

Stepniewska, I., Qi, H. X., & Kaas, J. H. (2000). Projections of the superior colliculus to subdivisions of the inferior pulvinar in New World and Old World monkeys. *Visual Neuroscience*, *17*, 529–549.

Sukekawa, K. (1988). Reciprocal connections between medial prefrontal cortex and lateral posterior nucleus in rats. *Brain, Behavior and Evolution*, *32*, 246–251.

Takahashi, T. (1985). The organization of the lateral thalamus of the hooded rat. *The Journal of Comparative Neurology*, *231*, 281–309 Retrieved from http://doi.wiley.com/10.1002/cne.902310302

Tohmi, M., Meguro, R., Tsukano, H., Hishida, R., & Shibuki, K. (2014). The Extrageniculate visual pathway generates distinct response properties in the higher visual areas of mice. *Current Biology*, *24*, 1–11. Retrieved from https://doi.org/10.1016/j.cub.2014.01.061

Wang, Q., & Burkhalter, A. (2007). Area map of mouse visual cortex. *The Journal of Comparative Neurology*, *502*, 339–357 Retrieved from http://doi.wiley.com/10.1002/cne.21286

Zhou, N., Maire, P. S., Masterson, S. P., & Bickford, M. E. (2017). The mouse pulvinar nucleus: Organization of the tectorecipient zones. *Visual Neuroscience*, *34*, E011 Retrieved from https://www.cambridge.org/core/product/identifier/S0952523817000050/type/journal_article

Zhuang, J., Ng, L., Williams, D., Valley, M., Li, Y., Garrett, M., & Waters, J. (2017). An extended retinotopic map of mouse cortex. *Elife*, *6*, 1171–1179 Retrieved from http://www.ncbi.nlm.nih.gov/pubmed/28059700

How to cite this article: Juavinett AL, Kim EJ, Collins HC, Callaway EM. A systematic topographical relationship between mouse lateral posterior thalamic neurons and their visual cortical projection targets. *J Comp Neurol*. 2019;1–13. https://doi.org/10.1002/cne.24737